Molecular Simulation Study of Tetraalkylammonium Halides. 1. Solvation Structure and Hydrogen Bonding in Aqueous Solutions

Joseph T. Slusher[†] and Peter T. Cummings*

Department of Chemical Engineering, University of Tennessee, 419 Dougherty Engineering Bldg., Knoxville, Tennessee 37996-2200 and Chemical Technology Division, Oak Ridge National Laboratory Oak Ridge, Tennessee 37831-6268

Received: October 24, 1996; In Final Form: February 10, 1997[⊗]

The hydration structure in aqueous solutions of three tetraalkylammonium halides (TAAX), tetramethylammonium chloride (TMACl), tetrapropylammonium bromide (TPABr), and tetrabutylammonium bromide (TBABr) at concentrations of 2.2, 1.4, and 1.0 *m*, respectively, is studied via molecular dynamics (MD) simulation at ambient conditions. The results are compared directly with neutron diffraction with isotopic substitution (NDIS) experimental results for the same systems. In agreement with the NDIS results, we find evidence of a small enhancement of water structure around the apolar solutes, based on water H−H radial distribution functions. Decomposition of the water−water O−H radial distribution function into hydrogen-bonded and non-hydrogen-bonded components, using the geometric criterion for hydrogen bonding of Mezei and Beveridge (1981), allowed us to calculate the hydrogen-bonded (HB) contribution to the total O−H radial distribution function, both in the bulk solution and in the first solvation shell of the cations. For the TPA and TBA cations, there is a small enhancement in the probability of forming hydrogen bonds between solvation shell water molecules, while the reverse is true for TMA. We find that the HB contribution to the total O−H coordination number remains approximately constant in going from pure water to the TAAX solutions. An analysis of the distributions of the parameters of the hydrogen-bonding criterion between pure water and water in the first solvation shells of the cations reveals that there is a slight tendency for the water in the first solvation shell to form more "ideal" hydrogen bonds compared to pure water, particularly for the the larger cations. However, the differences in the water−water structure between TPA and TBA are negligibly small.

1. Introduction

The study of the physical properties of apolar solutes in water can be traced in part to the work of Kauzmann, who reviewed the role of apolar interactions with regard to protein folding and stability in 1959.[1] Driven by the conjecture that hydrophobic effects may be the dominant interaction governing self-assembly phenomena in aqueous solution of organic molecules, the ensuing decades have seen intensive efforts to try to understand the nature of solvation in these solutions. In spite of the enormous research effort in this area, our basic understanding of the role of water−solute interactions, where the solute contains both polar and apolar regions, is far from complete. The central importance of the structural effects in aqueous solutions of apolar solutes as they relate to, for example, protein engineering, micelle formation, and molecular recognition phenomena is widely recognized. Such effects are usually discussed in terms of "hydrophobic hydration"which derives from the well-known characteristic properties of these solutes in water, *i.e.*, their low solubilities which reach a minimum with temperature near room temperature,[2] and their large positive heat capacity changes upon solvation.[3] The classical explanation of the above thermodynamic observations, which can be attributed to large negative entropies of solvation, is embodied in the concept of "iceberg" formation about apolar solutes in aqueous solution, introduced by Frank and Evans,[4] where the presence of the solute leads to a promotion in the structure of the neighboring water molecules analogous to that seen in ice. Subsequent "hydrophobic interactions" between apolar groups are usually thought of as resulting from a partial reversal of the solvation process, whereby the exposure of apolar groups to the water, and thus the unfavorable entropic contribution to the free energy of solvation, is minimized. The conjecture of an icelike structure around apolar solutes in water is sensible not only with regard to the hydration entropies but also in light of the analogous situation in crystalline water/apolar solute mixtures. Here, the residual effects of the enclosure of apolar solutes by stabilized water cages formed around them known as "clathrate hydrates" have been postulated to exist in the liquid state.[3]

The symmetric tetraalkylammonium halides (TAAX, X = Cl, Br, etc.) were early on identified as ideal models for studying hydrophobic phenomena, in part because their large solubilities in water allow concentrated solutions to be studied. They have the additional advantage that, without changing the overall shape of the molecule, one can unambiguously test the effects of changing the length of the alkyl chains, and thereby changing the ratio of polar to apolar groups, on their thermodynamic properties. They are also known to form clathrate hydrates in aqueous solution.[5,6] As models for hydrophobic effects, the solution properties of the tetraalkylammonium halide series have been the subject of intense research for more than three decades (see refs 7 and 8 for reviews of some of the relevant literature prior to 1973). The early thermodynamic, transport, and spectroscopic studies were not in agreement as to the structure of these solutions, although the indirect evidence pointed strongly to an ordering effect on the water by these salts.[7] The question of hydrophobic interaction between TAA cations in aqueous solutions has also been addressed both experimentally by small-angle neutron scattering (SANS),[9] NMR,[10] volumetric measurements,[11,12] and theoretically[13,14] with ambiguous results,

[†] Present address: Division of Physical and Chemical Properties, National Institute of Standards and Technology, Gaithersburg, MD 20899.

[⊗] Abstract published in *Advance ACS Abstracts,* April 15, 1997.

S1089-5647(96)03304-4 CCC: $14.00

although cationic pairing has been conclusively found for tetraphenyl-substituted ions in water.[15]

While the widely accepted conjecture of increased water structure is intuitive in explaining, in particular, the thermodynamic measurements, much of the current interest stems from a reconsideration of the role of water−water interactions in solvation entropies and attempts to unambiguously ascribe the thermodynamic behavior of these solutions to specific structural features. However, the role of water−water interactions in hydrophobic phenomena is still a matter of considerable debate. More recent measurements of, for example, transport entropies[16] and Raman spectra,[17] have been interpreted in support of the "structure-making" ability of the larger TAA salts, though others (infrared spectroscopy[18] and NMR[19]) have interpreted the experimental results without resorting to "structure making" ("breaking") concepts. Theoretical treatments and simulation studies have likewise yielded results which both support[20−25] and oppose[19,26−28] the notion of enhanced water−water interactions near apolar solutes.

In principle, examination of the partial pair correlations for water can shed direct quantitative light on the structural changes in water−water correlations in solutions of apolar solutes, particularly for those having large solubilities such as alcohols and the tetraalkylammonium halides. These are most directly obtained experimentally via neutron diffraction with isotopic substitution (NDIS), which typically gives orientationally averaged radial distribution functions (rdf's), although it is also possible to extract some orientational information.[29]

With the goal of looking for evidence of enhanced water−water correlations due to the presence of the tetraalkylammonium halide, using NDIS, Turner, Soper, and Finney[30−34] systematically studied aqueous solutions of tetramethylammonium (TMA), tetrapropylammonium (TPA), and tetrabutylammonium (TBA) halides in aqueous solution, focusing on the partial pair correlations between water−water, water−cation, and cation−cation. The overall conclusion from their work is twofold. In comparison to bulk water, water−water hydrogen−hydrogen rdf's, $g_{HH}(r)$, showed that the presence of TPABr and TBABr at fairly high concentrations (1.0−1.4 *m*) results in, at most, a small increase in the water−water structure. Comparison between TPABr and TBABr solutions showed that, in contrast to the significant differences in their thermodynamic behavior, there is very little difference in the average water structure around these cations. The implications of these results are that the structural enhancement of water commonly associated with hydrophobic hydration is only a minor effect and furthermore that an increase in water−water structure is not likely to be a major contributor to the large negative entropies of solution of these salts in water.

In the present work, molecular dynamics (MD) simulations are used to obtain a more detailed molecular picture of the microstructure of model solutions of three tetraalkylammonium halides: TMACl, TPABr, and TBABr in water. The simulations were performed at constant *N*, *V*, and *T* using experimental densities and potentials constructed from the literature. The salt concentrations were chosen to correspond to the experimental NDIS conditions in order to facilitate direct comparison of simulation to experiment. For TMACl, TPABr, and TBABr, the salt:solvent mole ratios were 1:25, 1:41, and 1:56, concentrations which are expected to give one independent layer of water around each cation.[17,34] Although we also present some of the more readily calculated thermophysical properties of these solutions, our main focus is on structural properties. We employ a geometric criterion for hydrogen bonding[35,50] in order to examine the hydrogen-bonding characteristics of water in the first solvation shell of the cations, with comparisons to the bulk solution water and pure water. In particular, some of the questions we seek to answer are the following. What effect, if any, is there of water on the conformation of the alkyl chains of these salts (particularly TBA), and what are the ion-paring characteristics in these solutions? Are there observable differences in the hydrogen-bonding characteristics of water in the first solvation shell of the cations, compared to those of bulk water in the solution and pure water? And finally, how well do the intermolecular potentials, constructed from the literature, represent the structural properties of the TAA halide solutions, *i.e.*, are the simulation results in agreement with the NDIS data?

TABLE 1: Geometrical Parameters for Molecular Models

molecule	bond length (Å)		bond angle (deg)	
water	O−H	1.000	HOH	109.47
TAA	C−N	1.510	CNC	109.50
	C−C	1.530	NCC	115.00
			CCC	109.47

TABLE 2: Pair Potential Parameters

molecule	group	σ (Å)	ϵ/k_b (K)	q
water	O	3.166	77.92	−0.82
	H	0	0	0.41
TAA	N	3.250	85.534	0
	CH_2−N	3.960	72.956	0.25
	CH_2, CH_3	3.960	72.956	0
Br	Br	5.040	32.520	−1.00

2. Simulation Methodology

2.1. Intermolecular Potentials. The inter- and intramolecular potentials used in this work were taken directly from the literature. For water, we used the simple point charge (SPC) model of Berendsen.[36] Jorgensen's model[37] was used for the tetraalkylammonium cations, in which the positive charge is distributed evenly among the four CH_2 groups attached rigidly to a central nitrogen. The alkyl chains of the cations were modeled using the potential of Ryckaert and Bellemans,[38] modified to include an angle-bending potential developed by Böcker *et al.*:[39]

$$u^{\text{bend}} = {}^1/_2 c_\theta(\theta - \theta_0)^2 \tag{1}$$

where $c_\theta/k_b = 526.89$ K is a constant and $\theta_0 = 109.47°$ is the equilibrium bond-angle. Their work also includes a 3-fold symmetrical potential used to describe rotation about the four $N-CH_2-CH_2-CH_2$ bonds,

$$u^{\text{rot}} = -c(1 - \cos 3\varphi) \tag{2}$$

where $c/k_b = 455.58$ K. For the cations, there is also an intramolecular Lennard-Jones (LJ) interaction between sites separated by more than three bonds. For bromide, we used the potential of Pálinkás *et al.*[40] All of the above intermolecular potentials are pairwise additive site−site Lennard-Jones plus Coulombic potentials,

$$u_{i\alpha j\beta} = u_{i\alpha j\beta}(r_{i\alpha j\beta}) = 4\epsilon_{i\alpha j\beta}\left\{\left(\frac{\sigma_{i\alpha j\beta}}{r_{i\alpha j\beta}}\right)^{12} - \left(\frac{\sigma_{i\alpha j\beta}}{r_{i\alpha j\beta}}\right)^{6}\right\} + \frac{q_{i\alpha}q_{j\beta}}{r_{i\alpha j\beta}} \tag{3}$$

where $u_{i\alpha j\beta}$ is the potential energy between site α on molecule *i* and site β on molecule *j*, and $q_{i\alpha}$ is the partial charge on site α of molecule *i*. The Lennard-Jones size (σ) and energy (ϵ) parameters between unlike sites were obtained using the Lorentz−Berthelot combining rules, *i.e.*, $\epsilon_{i\alpha j\beta} = (\epsilon_{i\alpha j\beta})^{1/2}$, $\sigma_{i\alpha j\beta} = (\sigma_{i\alpha} + \sigma_{j\beta})/2$. Molecular geometries are given in Table 1, and the parameters for eqs 1−3 are given in Table 2.

TABLE 3: Simulation Details

solute	N_s:N_w	ρ (g/cm^3)	T (K)	run length (ps)
water		1.0	298.0	102
TMACl	10:250	1.0	298.0	204
TPABr	6:252	1.0	298.0	1020
TBABr	4:228	1.0	298.0	1020

2.2. Equations of Motion. The equations of motion for site α of molecule i are Newton's equations modified to include intramolecular constraint forces necessary to maintain rigid bond length constraints:

$$\dot{\mathbf{p}}_{i\alpha} = m_{i\alpha}\ddot{\mathbf{r}}_{i\alpha} = \mathbf{F}^{\mathrm{N}}_{i\alpha} + \mathbf{F}^{\mathrm{C}}_{i\alpha} + \xi\mathbf{p}_{i\alpha} \tag{4}$$

where m, $\mathbf{r}$, and $\mathbf{p}$ are the mass, position, and linear momentum, $\mathbf{F}^{\mathrm{N}}$ is the sum of nonbonded forces due to the other sites $j\beta$ and intramolecular forces due to bending and torsion, $\mathbf{F}^{\mathrm{C}}$ is the constraint force needed to enforce rigid bond-length constraints and obtained noniteratively within the framework of the Beeman variant of the velocity−Verlet algorithm,[41] and ξ is a thermostating variable which changes with time according to[44]

$$\xi = \nu^2_{\mathrm{T}}\left(\frac{K(t)}{K_{\mathrm{set}}} - 1\right) \tag{5}$$

Here K_{set} is the kinetic energy of the system corresponding to the set-point temperature, $K(t)$ is the instantaneous kinetic energy based on the momenta of all sites, and ν^2_{T} is a thermostating rate set equal to 1000. We used the Ewald summation method with infinitely conducting boundary conditions[42,43] to handle long-ranged Coulombic interactions. The convergence parameter κ[45] was set at a value of 0.277 Å^{-1}, and 337 reciprocal lattice vectors were used. Both the Lennard-Jones interactions and real space part of the Ewald potential were cut off at 8.6 Å. No long-range corrections were included for the LJ interactions. The equations of motion were integrated as described in ref,[41] using a time-step size of 1.02×10^{-3} ps. In order to speed up the calculations, we used PVM[46] in conjunction with the data replication scheme and performed the simulations on an IBM SP2, a network of Silicon Graphics workstations using four processors, and on an Intel Paragon at Oak Ridge National Laboratory. The simulations were run at constant density and temperature, using densities obtained experimentally.[47−49] The system sizes (232−270 molecules) and additional simulation details are given in Table 3.

2.3. Hydrogen Bonding. To quantify the hydrogen bonding in the solutions, we use the minimal geometric criterion of Mezei and Beveridge,[35,50] which is given in terms of four internal coordinates fixed by the relative positions of two water molecules (see Figure 1). These are the O···O separation distance and three angles describing respectively the H−O···O angle, (θ_{H}), the lone-pair (LP)−O···O angle (θ_{LP}), and the dihedral angle between the planes H−O···O and LP−O···O (δ_{D}). With this criterion, two water molecules are considered to be hydrogen bonded if $R_{\mathrm{OO}} \le 3.3$ Å, θ_{H}, $\theta_{\mathrm{LP}} \le 70.53°$, and $\delta_{\mathrm{D}} \le 180°$. Using the above definition, the total OH radial distribution function can be divided into two contributions: one from water molecules that are within the limits of the above criterion at arbitrary separation r, $g^{\mathrm{HB}}_{\mathrm{OH}}(r)$, and the other from those which are in a configuration other than hydrogen bonding, $g^{\mathrm{NHB}}_{\mathrm{OH}}(r)$. From consideration of the configurational space volume,[35,50] we have[51]

$$g_{\mathrm{OH}}(r) = {}^1/_9 g^{\mathrm{HB}}_{\mathrm{OH}}(r) + {}^8/_9 g^{\mathrm{NHB}}_{\mathrm{OH}}(r) \tag{6}$$

and thus the total coordination number $n_{\mathrm{OH}}(r)$ is a sum of two contributions, *i.e.*,

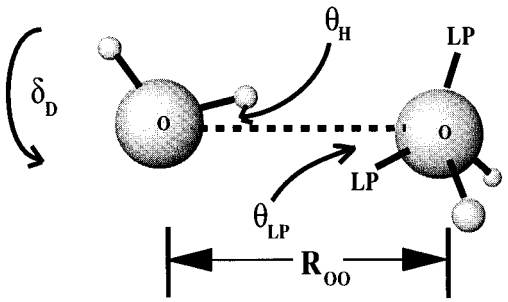

Figure 1. Schematic of hydrogen-bonding parameters.

$$n_{\mathrm{OH}}(r) = n^{\mathrm{HB}}_{\mathrm{OH}}(r) + n^{\mathrm{NHB}}_{\mathrm{OH}}(r) = \frac{4\pi\rho x_{\mathrm{H}}}{9}\int_0^r g^{\mathrm{HB}}_{\mathrm{OH}}(r) r^2\,\mathrm{d}r + \frac{32\pi\rho x_{\mathrm{H}}}{9}\int_0^r g^{\mathrm{NHB}}_{\mathrm{OH}}(r)\, r^2\,\mathrm{d}r \tag{7}$$

3. Simulation Results

3.1. Thermodynamic Results. The energetic results of the calculations are given in Tables 4 and 5, where we also show the component-wise contribution to the total energy for both the LJ and Coulombic parts of the interactions. Unfortunately, it is possible to obtain only estimates of the specific electrostatic interactions because of the effective screening of the partial charges when using the Ewald sum. Nevertheless, a trend can be seen which shows water−water Coulombic interactions becoming more favorable while the reverse is true for water−cation interactions as the cation size increases. The small negative TMA^+−water interaction energy agrees qualitatively with the results of Jorgensen and Gao for an isolated TMA ion in water. The TMA^+ $-Cl^-$ LJ and Coulombic interactions suggest the formation of contact ion pairs in this concentrated solution, though these appear to be less favorable for the TPABr and TBABr solutions. Also shown in Table 4 are water self-diffusion coefficients in the three solutions, obtained from the Einstein formula.[45] These results show water translational motion is hindered in these solutions compared to bulk water, in line with experimental NMR studies of TAAB[52,53] and TAACl.[10] Although the relative change in D_{w} compared to pure water agrees well with the experimental data for the TMACl solution,[10] it is largely underestimated for the larger salts.

3.2. Cation Conformations and Ion−Ion Interactions. To show the average conformation of the flexible cations in water, we plot the end-to-center distance probability for TPA^+ and TBA^+ in water in Figure 2. Whereas the alkyl chains on the TPA ion are entirely trans, for the TBA cation there is some contribution from gauche conformers in the last dihedral angle (*i.e.*, farthest from the N), although the others are on average predominantly in the fully stretched, trans conformation. Integration of these dihedral angle distributions for TBA indicates the ratio of trans to gauche conformers is 73:27. The predominantly trans conformation of the alkyl chains in TBA is in agreement with predictions based on various thermodynamic measurements[7] as well as small-angle neutron scattering measurements.[9] The ratio of trans to gauche in the last dihedral angle is, however, significantly higher than would be the case for an isolated butane in 216 water molecules, where Monte Carlo calculations predict the ratio of *trans*- to *gauche*-butane to be 56:44 and is even higher than the ideal gas value of 68:32.[37]

A number of studies have suggested that the variation in dissociation constants with ion size for the TAA halides in water follows the reverse trend as is found with aqueous inorganic salts, for which ion pairing is more pronounced as the both the cations and/or anions become smaller.[56−58] This information

TABLE 4: Thermodynamic Results[a]

solute	D_w[b]	K	U^c	U^{rot}	U^{bend}	U^{intra}	U^{tot}
water	3.5(1)	7.44(1)	−41.9(1)				−34.4(1)
TMACl	2.8(1)	7.76(1)	−58.3(1)				−50.5(1)
TPABr	3.0(1)	8.33(3)	−51.1(2)	5.9(1)	10.4(1)	−10.9(1)	−42.6(1)
TBABr	2.9(1)	8.35(1)	−48.72(5)	15.5(2)	15.6(1)	−14.22(3)	−40.08(5)

[a] U^c and U^{tot} are configurational and total energy in kJ (mol of water + mol of salt)$^{-1}$. Bending torsional, and intramolecular energies in kJ (mol of salt)$^{-1}$. [b] Units of 10^{-9} m^2 s^{-1}.

TABLE 5: Averaged Pairwise Energies[a]

solute	W−W	W−C	W−A	C−C	C−A	A−A
			Lennard-Jones			
water	7.43(6)					
TMACl	7.18(5)	−0.91(3)	1.63(4)	−1.6(4)	1.3(5)	−0.07(1)
TPABr	7.17(4)	−1.70(4)	0.80(1)	−6(1)	−1.2(1)	−0.05(1)
TBABr	7.21(1)	−1.72(2)	0.60(1)	−8.3(8)	−1.5(3)	−0.03(1)
			Coulombic[b]			
water	−46.6(1)					
TMACl	−38.5(4)	−1.5(2)	−11.2(3)	1.8(6)	−23(3)	2.5(6)
TPABr	−40.4(2)	−0.90(4)	−6.1(1)	0.4(1)	−7(1)	0.8(3)
TBABr	−41.5(1)	−0.80(4)	−4.9(1)	0.24(8)	−5(2)	0.7(4)

[a] Solvent−solvent interactions are given in kJ (mol of solvent)$^{-1}$. Solvent−ion interactions in kJ (mol of salt + solvent)$^{-1}$. Ion−ion inteactions in kJ (mol of salt)$^{-1}$. [b] Shielded partial charges.

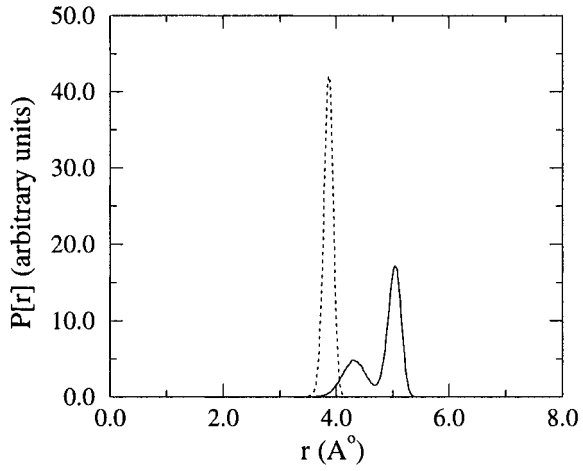

Figure 2. Probability distribution of salt center−alkyl chain end distance: (···) TPABr; (—) TBABr.

is also useful as the degree of ion pairing can be expected to have some influence on the hydration structure around the cations. In the case of strictly dimer formation between unlike ion pairs, the tendency for cation−anion ion pair formation can be quantified by calculating the degree of dissociation α of the salt, defined as the ratio of free ions to the total number in the solution. In this case, for a 1−1 electrolyte, the number density of free cations and anions, ρ_C and ρ_A, is

$$\rho_C = \rho_A = \rho_{C0} - \rho_{CA}, \quad \rho_{A0} = \rho_{C0} = \rho_0 \tag{8}$$

where ρ_0 is the number density of the salt, and therefore

$$\alpha \equiv \frac{\rho_C}{\rho_0} = \frac{\rho_A}{\rho_0} = 1 - \frac{\rho_{CA}}{\rho_0} \tag{9}$$

If the cation−anion pair is considered to be associated when $0 < r_{CA} \leq r_2$, where r_2 is the upper bound of the cation−anion solvation shell (usually taken as the first minimum in the center-of-mass cation-anion rdf, $g_{CA}(r)$), then for the number density of cation−anion pairs we have[59,60]

$$\rho_{CA} = 4\pi\rho^2 \int_0^{r^2} g_{CA}(r) r^2 \, dr \tag{10}$$

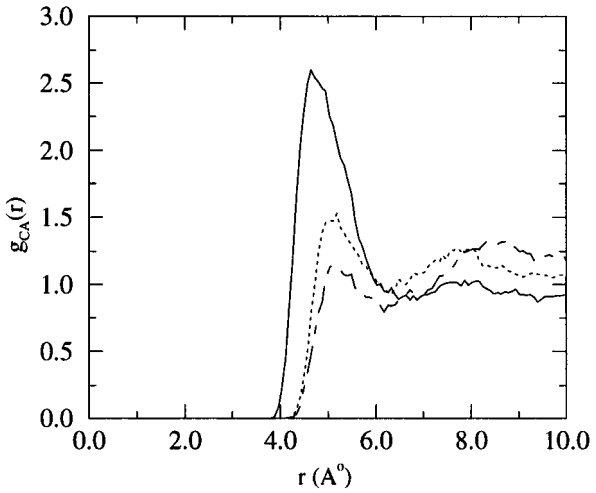

Figure 3. Cation−anion center-of-mass radial distribution functions, $g_{CA}(r)$: (—), TMACl; (···) TPABr; (− - −) TBABr.

and so the degree of dissociation, α, is given by

$$\alpha = 1 - 4\pi\rho_0 \int_0^{r^2} g_{CA}(r) r^2 \, dr \tag{11}$$

An accurate determination of α would then require either simulation of a dilute solution of very large system size to obtain adequate statistics or indirect evaluation via potential of mean force calculations, as has been done for an isolated TMA−Cl pair in water.[37] In the present case, since the salt concentrations are relatively large, we have to consider the possibility of higher order ion−ion association, and, possibly cation−cation pair formation. Then the concentration of free cation, for example, is

$$\rho_C = \rho_{C0} - \rho_{CA} - 2\rho_{CC} - \rho_{CAA} - 2\rho_{CCA} - \ldots \tag{12}$$

and the simple formulas of eqs 10 and 11 would no longer be valid. For example, higher order correlation functions are needed to deconvolute contributions to $g_{CA}(r)$ from higher-order complexes.

These higher-order correlation functions could be estimated using the Kirkwood superposition approximation[26] and the unlike- and like-ion rdf's. In the present calculations, however, the small system sizes do not allow accurate determination of these rdf's, and we can obtain only estimates of α from direct integration of $g_{CA}(r)$ (Figure 3) in eq 11. For the TPABr and TBABr solutions, eq 11 yields 0.50 (6.35 Å) and 0.74 (6.18 Å), respectively, where r_2 is given in parentheses. For the TMACl solution, we obtain −0.37 (6.32 Å), indicating that for this system the presence of higher order ion−cluster formation is significant. The trend of decreasing attraction between unlike ions with increasing cation size predicted by the simulations appears to disagree with many data indicating that TAAX ion pairs become more stable as both the cation and anion become larger.[56] However, we note that the salt concentrations in the present simulations are relatively large and are increasing in such a way as to mask any evidence of this trend, even if it can be predicted with the molecular models employed in the present calculations.

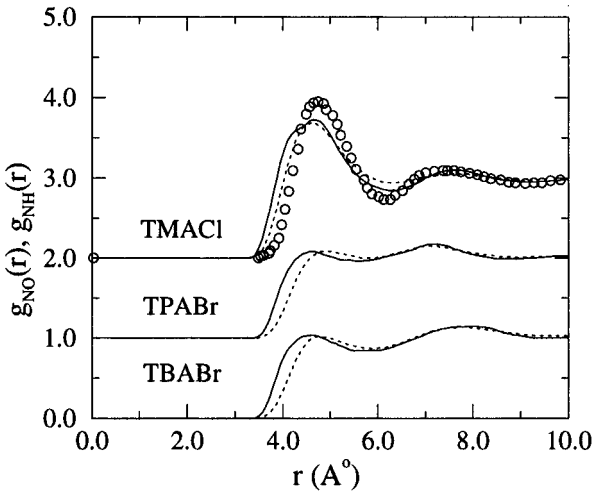

Figure 4. Cation−water N−O_w (—) and N−H_w (···) radial distribution functions. (○) NDIS results for center-of-mass TMA−water.[29]

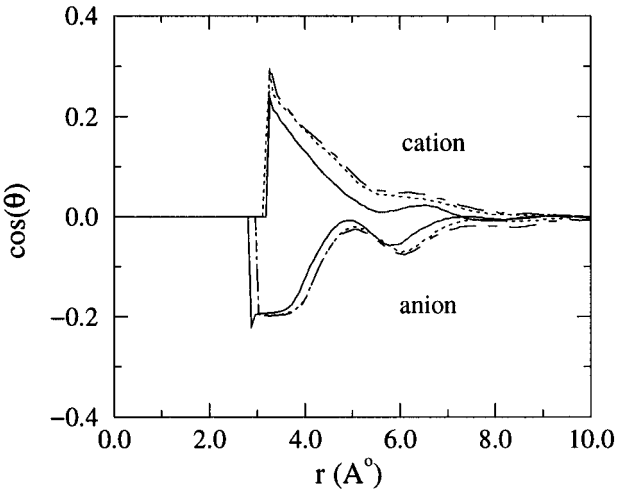

Figure 5. Orientation of permanent water dipole with respect to ion centers: (—) TMAB; (···) TPABr; (− - −) TBABr.

3.3. Ion−Water Interactions. Some information about the orientation of water with respect to the center of the ions can be obtained from the N−O_w and N−H_w rdf's, shown in Figure 4. The cation-water rdf's indicate that on average, for all three salts, the water molecules are located nearly tangentially with respect to the center of the cations, with both N−O_w and N−H_w distances nearly the same, although the oxygens are on average about 0.2 Å closer to the cation center. These findings are in agreement with other simulations,[20,22,62−64] which indicate that the water is oriented around apolar solutes in such a way as to maximize H bonding with the surrounding water. Similarity in the N−O_w and N−H_w distances is also not incompatible with the suggestion of a clathrate-like arrangement of the water molecules around the cations. The TMA−water rdf's agree closely with the results of Impey and Klein[7] for an isolated TMA ion in water and are also in good agreement with the center-of-mass TMA−water radial distribution function obtained via NDIS,[29] also shown in the figure. The agreement between the NDIS and simulation results for the TMA N−O_w rdf gives a good indication that the potentials used are adequate to describe the structure of these solutions. Interestingly, though there are large differences in the size of the cations, the distances of closest approach of the water are nearly invariant at about 3.3 Å, as are the locations in the first peaks of $g_{NO}(r)$. The peak heights, however, are decreased substantially for the larger cations and, as suggested by the energies, indicate that the electrostatic attraction between the cations and water is becoming less important as the cation size increases. Considering the radii of the cations (Figure 2), it is evident that the water molecules comprising the first hydration shell of the TPA and TBA ions reside almost entirely in the spaces between the alkyl chains.

Further information about the orientation of the water molecules around the ions is obtained by examining the average angle between the bisectrix of the H−O−H angle and the vector joining the center of the ion with the water oxygen

$$\cos\theta = \hat{\mathbf{r}}_{ON}\cdot\hat{\mathbf{r}}_b \qquad (13)$$

where $\mathbf{r}_{ON} = \mathbf{r}_O - \mathbf{r}_N$, and $\mathbf{r}_b$ points from the oxygen to the point between the hydrogens. In Figure 5, we show how the cosine of this angle changes with ion−water distance for the three different cations and for bromide and chloride. Around the anions, water in the first solvation shell (∼3−4 Å, see Figure 6) maintains a nearly constant orientation, with an anion···O−H angle of 25−30°. Hydrogen bonding between the first and second hydration shell waters is also clearly manifested in the second peak centered at about 6 Å. Consistent with the cation−O_w and H_w rdf's, the orientation of the permanent water dipole around the cation is similar among the three cations. In contrast to the orientations around the anions, however, there is a much wider variation in the water orientation within the first solvation shell and a more shallow peak corresponding to the second shell water. The HOH bisector of water around the cations is nearly tangential and becomes almost completely so near the outer edge of the first solvation shell. Such a configuration is consistent with "apolar" (as opposed to ionic) hydration and allows a surrounding water molecule to maintain three of the four hydrogen bonds it would otherwise (on average) be involved in. The water around TMA shows a greater tendency to orient its HOH bisector tangentially as compared to the situation around the larger cations. Interestingly, the orientation angle θ is nearly invariant between the TPA and TBA cations. Here, the greater tendency (relative to TMA) of water between the alkyl chains of TPA and TBA to orient its hydrogens more toward the bulk must be due to the presence of the longer alkyl chains, which would tend to make purely tangential orientations with respect to the cation center less favorable.

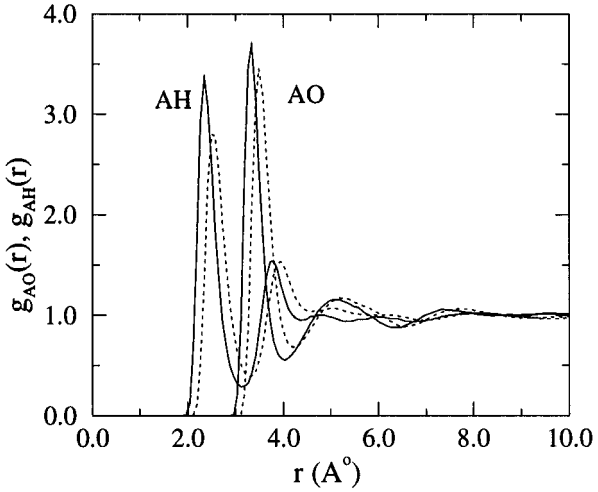

Figure 6. Anion−water Cl−O_w, Cl−H_w, Br−O_w, and Br−H_w radial distribution functions for TMACl (—) and TPABr (···) solutions.

3.4. Water−Water Interactions. *3.4.1. H_w−H_w Correlations.* The H_w−H_w radial distribution functions for water in the TBABr/water solution are compared with the experimental NDIS results in Figure 7. The effect of the other salts is similar. In qualitative agreement with the NDIS results, we find that the solution water H_w−H_w structure is similar to pure water, the effect of the solutes on $g_{HH}(r)$ being to uniformly increase

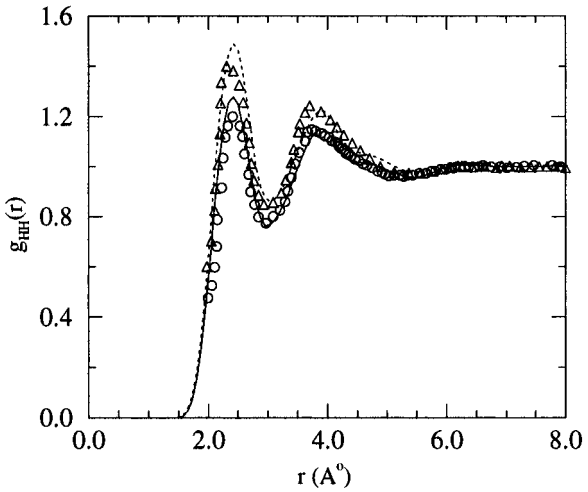

Figure 7. Water−water H_w-H_w radial distribution functions in pure water (—) and 1.0 *m* TBABr (···) solution compared to experiment (symbols): (○) pure water; (△) 1.0 *m* TBABr in water.[34]

TABLE 6: Water−Water H−H Coordination Numbers Compared to NDIS[a]

solute	ρ_w[b]	$n_{H,exp}^{(H)}$	r_2	$n_{H,sim}^{(H)}$[c]
water	3.33	4.8(1)	3.00	5.94
TMACl	2.69		3.04	5.46
TPABr	2.48	4.5(2)	3.06	5.46
TBABr	2.43	4.4(2)	3.06	5.56

[a] Reference 34. [b] Units of ρ are 10^{-2} molecules Å^{-3}. [c] Uncertainties in coordination numbers are ≈0.01.

the height of the correlation functions. The uniform increase in $g_{HH}(r)$ at small r can be understood in light of the coordination number of site β around site α,

$$n_\beta^{(\alpha)} = 4\pi\rho x_\beta \int_0^{r_2} g_{\alpha\beta}(r) r^2 \, dr \qquad (14)$$

where r_2 is the first minimum in $g_{\alpha\beta}(r)$. Since ρx_H is smaller in the solution compared to pure water, an increase in $g_{HH}(r)$ in the solution would be necessary in order for water to maintain its pure water H_w-H_w coordination number, $n_H^{(H)}$. These values are compared for both water in the solutions and pure water to the experimental values in Table 6. Although not in quantitative agreement with the NDIS values, the same trend is seen; *i.e.*, the coordination numbers are decreased by about 0.4 compared to that of pure water.

3.5. Water−Water O−H Distributions. While H−H correlation functions are most easily obtained via NDIS experiments, more direct evidence of the degree of hydrogen bonding in aqueous solutions is available from the oxygen−hydrogen site−site rdf, and in particular, coordination numbers obtained via its volume integral. However, Chialvo and Cummings[51] recently pointed out that total coordination numbers based on $g_{OH}(r)$ may not in themselves be good indicators of the degree of hydrogen bonding in aqueous systems. This is because a substantial portion (about 50%, see Table 7) of the contribution to $n_H^{(O)}(r)$ at the first minimum in the function is from water pairs which are *not*, according to the Mezei−Beveridge criterion, in the correct orientation for hydrogen bonding. As a result, even for a water-like molecule having the same geometry of SPC water, but with partial charges reduced by a factor of ∼300, the total O−H coordination number at the first minimum in $g_{OH}(r)$ is very close to that of SPC water.[51] Introducing $g_{OH}^{HB}(r)$ allows one to look directly at the characteristics of the hydrogen bonding taking place, as well as the amount of H bonding taking place via its volume integral, thereby obtaining

TABLE 7: Water−Water O−H Coordination Numbers

solute	ρ_w[a]	ρ_w^{shell}[b]	$n_H^{(O)}$	$n_{H,HB}^{(O)}$	$n_H^{(O),shell}$	$n_{H,HB}^{(O),shell}$
water	3.33		1.96	0.99		
TMACl	2.69	3.25	1.71	0.88	1.01	0.53
TPABr	2.48	2.20	1.74	0.89	0.67	0.35
TBABr	2.43	2.11	1.75	0.90	0.74	0.39

[a] Units of ρ are 10^{-2} molecules Å^{-3}. [b] ρ_w^{shell} is obtained by dividing the coordination number of water around the cations by the volume of the solvation shell = $4\pi(R_0^3 - R_x^3)/3$ assuming a spherical volume for the cations of radius equal to the excluded volume R_x. R_0 is the position of the first minimum in $g_{CW}^{com}(r)$. The estimated values for R_x and R_0 are for TMACl, TPABr, and TBABr respectively (3.5,6.25), (3.3,5.65), and (3.3,5.8), in Å.

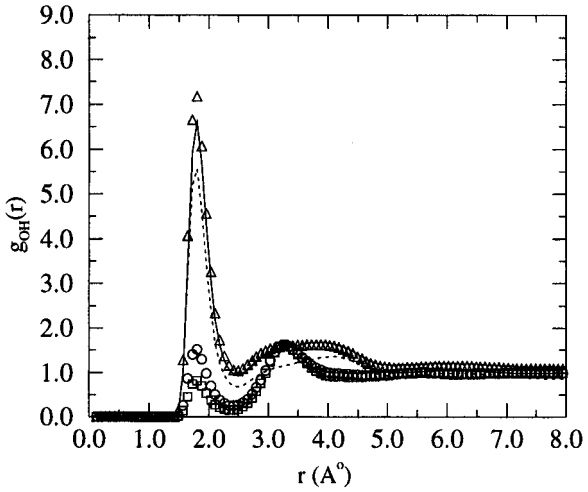

Figure 8. Water−water O−H radial distribution functions for bulk solution water (symbols) and water in first solvation shell of TMA (···) compared to pure water (—). (△) $g_{OH}^{HB}(r)$; (○) $g_{OH}(r)$; (□) $g_{OH}^{NHB}(r)$; (···) $g_{OH}^{HB}(r)$; (—) pure water $g_{OH}^{HB}(r)$.

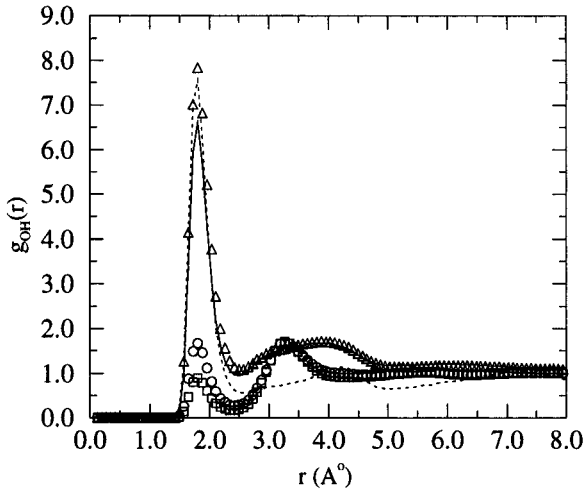

Figure 9. Water−water O−H radial distribution functions for bulk solution water (symbols) and water in first solvation shell of TPA (···) compared to pure water (—). (△) $g_{OH}^{HB}(r)$; (○) $g_{OH}(r)$; (□) $g_{OH}^{NHB}(r)$; (···) $g_{OH}^{HB}(r)$; (—) pure water $g_{OH}^{HB}(r)$.

an unambiguous picture of hydrogen bonding in these solutions. In Figures 8−10 we compare $g_{OH}(r)$, $g_{OH}^{HB}(r)$, and $g_{OH}^{NHB}(r)$ for the bulk solution water with $g_{OH}^{HB}(r)$ for water in the first solvation shell of the cations and for pure water. The procedure for calculating the rdf's between water molecules in the first solvation shell of the cation is outlined in the Appendix.

Looking first at the bulk solution water, a comparison of $g_{OH}^{HB}(r)$ for solution water with pure water shows that, similar to the results for $g_{HH}(r)$, the entire curves are raised slightly relative to the pure water result. However, the relative sharpness of

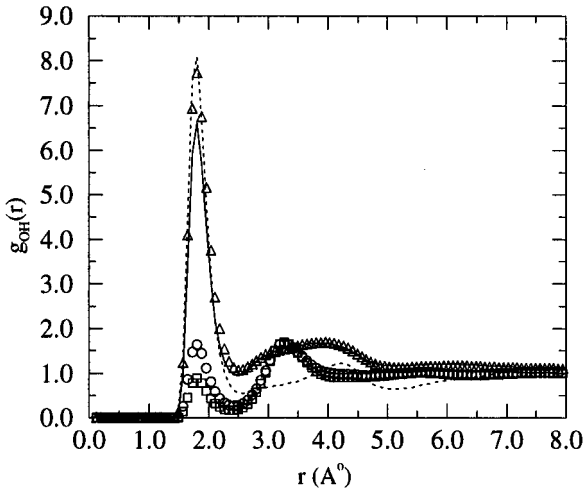

Figure 10. Water−water O−H radial distribution functions for bulk solution water (symbols) and water in first solvation shell of TBA (···) compared to pure water (—). (△) $g_{OH}^{HB}(r)$; (○) $g_{OH}(r)$; (□) $g_{OH}^{NHB}(r)$; (···) $g_{OH}^{HB}(r)$; (—), pure water $g_{OH}^{HB}(r)$.

the HB peaks appears to be slightly greater for the solutions compared to pure water, particularly for the larger cations.

In the case of the hydration shell distribution functions, $g_{OH}^{HB}(r)$ gives the probability of finding an O and an H a distance r apart on two water molecules within the hydrogen-bonding orientational criterion, relative to what would be expected if the water molecules were *oriented* randomly about the cations but distributed nonrandomly with respect to the cation according to $g_{CW}^{com}(r)$, the center-of-mass cation−water rdf. Because these shell distribution functions take into account the spatial rearrangement of the solvent to accommodate the cation, a direct comparison with $g_{OH}^{HB}(r)$ for pure bulk water is appropriate. For TMA, $g_{OH}^{HB}(r)$ in the cation hydration shell is smaller than that in pure water, while it is clearly somewhat enhanced in the TPA and TBA solutions. In that sense, we can say that degree of hydrogen bonding in the solvation shell of TMA is less than that in pure bulk water, while it is greater than that of pure water around the TPA and TBA cations although in all cases the effect is relatively small. The actual values of the O−H coordination numbers for the hydration shell waters, given in Table 7, are simply a reflection of both the average density of water around the cations and the loss of HB sites in the direction of the solute. They also do not include the hydrogen-bonding interactions between waters in the first with those in the second hydration shell.

Aside from the amount of hydrogen bonding taking place in the vicinity of the cations, one can also examine the characteristics of the hydrogen bonds. For this purpose, in Figures 11−14 we display the distribution of the four hydrogen-bonding parameters for hydrogen bonds between water molecules in the first solvation shell of the cations, as compared to the distributions in pure bulk water. The analysis of these results is complex. However, the main differences in the distributions of these parameters are toward more narrow distributions of the parameters, with the exception of the LP-O···O angle, θ_{LP}. This suggests that the hydrogen bonds forming between water molecules in the vicinity of the cations are, on average, somewhat more "ideal" than those of bulk water, in the sense that they are shorter and more linear in character.

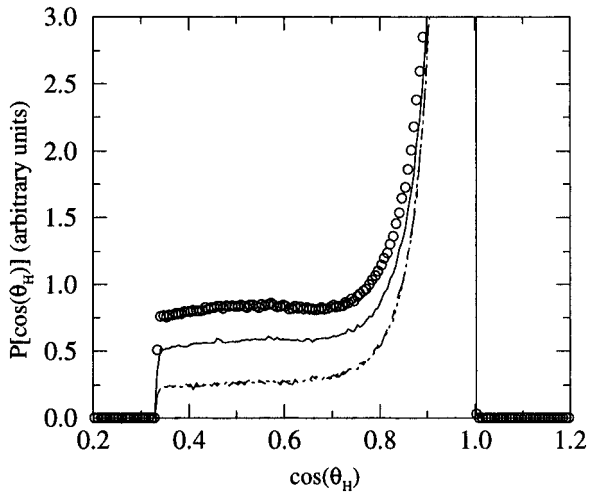

Figure 11. Distribution of hydrogen-bonding parameter θ_H in pure water compared to TAAX solution: (○) pure water; (—) TMACl; (···) TPABr; (− - −) TBABr.

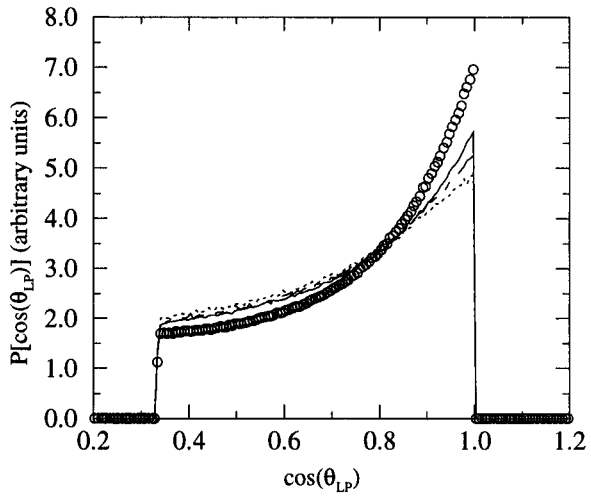

Figure 12. Distribution of hydrogen-bonding parameter θ_{LP} in pure water compared to TAAX solution: (○) pure water; (—) TMACl; (···) TPABr; (− - −) TBABr.

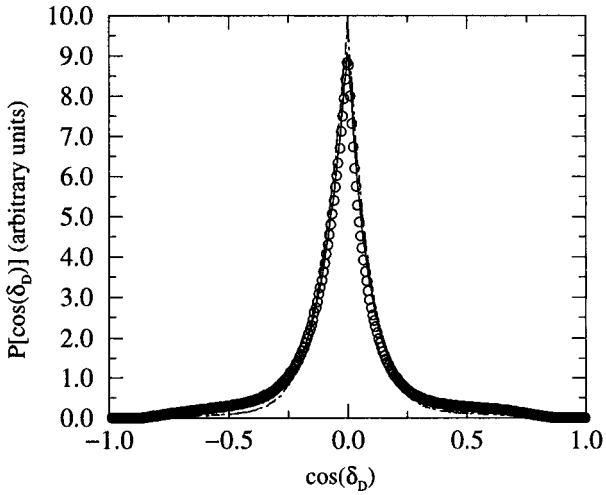

Figure 13. Distribution of hydrogen-bonding parameter δ_D in pure water compared to TAAX solution: (○) pure water; (—) TMACl; (···) TPABr; (− - −) TBABr.

4. Discussion and Conclusion

As prototypical models for hydrophobic effects, solutions of tetraalkylammonium halides in water have been the subject of a large number of experimental and several theoretical investigations, whose overall aim has been to link the microscopic structure of these solutions with the thermodynamic properties representative of hydrophobic hydration. In particular, the suggestion that the large TAA cations occupy cavities in water around which the water−water interactions are stabilized,

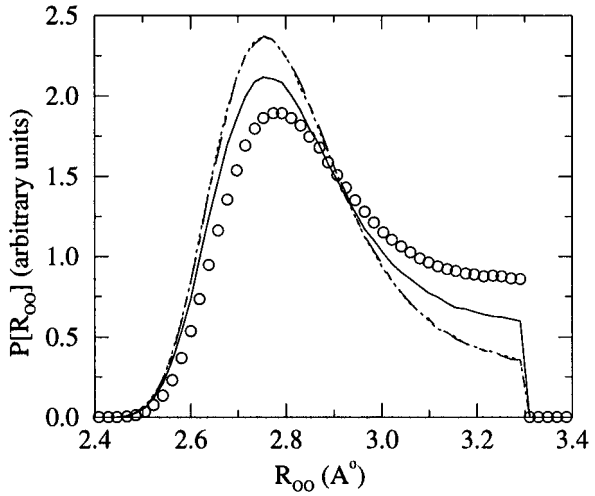

Figure 14. Distribution of hydrogen-bonding parameter R_{OO} in pure water compared to TAAX solution: (○) pure water; (—) TMACl; (•••) TPABr; (– - –) TBABr.

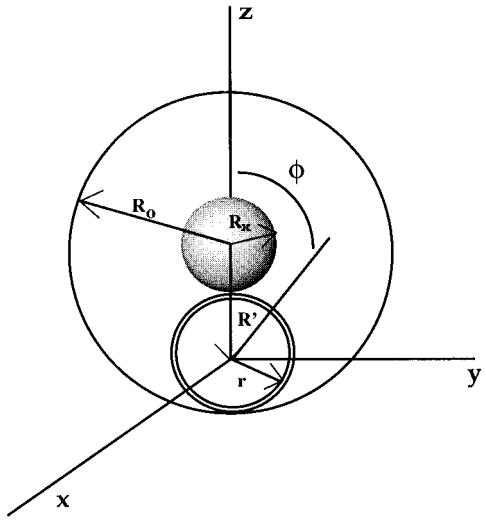

Figure 15. Schematic of solvation shell.

resulting in the large negative entropy losses seen experimentally, has remained an open question. Inasmuch as the sharpening of peaks in the site−site rdf's for bulk solution water is indicative of enhanced water−water interactions around the cations, our results, being in qualitative agreement with the NDIS results for TPABr and TBABr,[34] fully corroborate the conclusions based on that work, *i.e.*, that the larger TAA cations do in fact have a stabilizing influence on the water−water interactions, although the overall effect is small. In further agreement, the differences in the effects of the TPABr and TBABr cations with regard to rdf peaks and HB parameter distributions are very small, in contrast to the significant differences in their thermodynamic solution properties.

The TMA ion is, according to our results, fully associated at the concentration of the present simulation (∼2 *m*) and is located in a cavity of higher-than-bulk density water comprising its first solvation shell. At this concentration, all of the water molecules in the simulation are nearest neighbor to a TMA cation. The TPA and TBA, on the other hand, are only partially associated, and their first solvation shell water molecules, located between the alkyl chains, are a fraction of the total number in the solution. In these solutions, unlike in the TMACl solution, there is essentially no difference between the bulk hydrogen-bonding O−H rdf's and those of the cation solvation shells. Looking only at the rdf's for the bulk solution water, the results would indicate that all three cations enhance the hydrogen bonding slightly, although the effect is rather small for the TMACl solution. In the neighborhood (first solvation shell) of the TAA cations, there is obviously the possibility for fewer water−water hydrogen bonds to form due to the loss of a hydrogen-bonding opportunity in the direction of the cation, and, for TPA and TBA, steric hindrance of the alkyl chains to water penetration and the resulting decrease in the solvation shell water density (Table 7). This is reflected in the overall decrease in $n_{H,HB}^{(O)}$ in going from pure water to the solutions. However, taking into account the concentration of water near the cations as a function of radial distance from the cation centers, we have looked at the hydrogen-bonding probabilities between waters which *are* present in the first solvation shell of a given cation. For the larger cations, on the basis of $g_{OH}^{HB}(r)$ between waters in the neighborhood of the cations and its volume integral, we conclude that, between the water molecules which are adjacent to these apolar salts, the probability of hydrogen-bonding orientations is slightly greater relative to what it would be in bulk water. Between water molecules in the solvation shell of a given TMA cation, the reverse appears to be true. Within the context of the Mezei−Beveridge criterion for hydrogen bonding, the distributions of the four HB parameters appear to be shifting in such a way as to suggest that the hydrogen bonds forming between solvation shell waters are in some sense more "ideal" than those in pure bulk water, though less so in the TMACl solution. For that salt, the apolar/polar nature of the cation hydration structure has been found to be highly concentration dependent, perhaps due to the effect of chloride ions near the cation.[30] It would be interesting to extend these simulations to more dilute salt concentrations. Currently, formulation of a direct theoretical link between structural results such as those presented in this work and the hydration entropy of apolar solutes in water is an area of active research.[28, 65] In the meantime, the overall conclusion from the present results is that there appears to be at least a small contribution from water−water correlations to the large, negative hydration entropies found experimentally in these solutions. We are currently studying solvent effects on conformation and solvation structure in mixed water/2-propanol solutions of TAA bromides, to appear in a future publication.

Acknowledgment. The authors are grateful for financial assistance from the Office of Basic Energy Sciences, U.S. Department of Energy. We also thank the Center for Computational Sciences, Oak Ridge National Laboratory, for CPU allocations on the IBM SP2 and Intel Paragon computers. Our interest in tetraalkylammonium halide solutions originated in experimental measurements performed in collaboration with Professor John O'Connell of the University of Virginia.[47,48] We are grateful to Professor O'Connell for many stimulating discussions concerning these solutions.

Appendix

In the following we detail the method used to calculate the O_w-H_w radial distribution functions between water molecules in the first solvation shell of the cation (see Figure 15). The cation is treated as a sphere with radius given by the radius of the excluded volume, R_x, *i.e.*, the minimum distance at which $g_{CW}^{com}(r)$ becomes nonzero. To take into account the nonuniform distribution of water around the cations, the normalization of the $g^{shell}(r)$ histograms uses $\rho x_w\, g_{CW}^{com}(r)$ rather than the bulk water density, ρx_w. Given this information, for a water molecule located at an origin that is a fixed distance R' away from the center of the cation, the average number of water molecules in a spherical shell of thickness dr a distance r away from the water molecule at R' is

$$n_b^{shell}(r)|_{R'} = \rho x_w \int_0^{2\pi}\int_0^{\varphi 2}\int_{r-dr/2}^{r+dr/2} r^2\, g_{CW}^{com}(r_{CW})\, dr \sin\varphi\, d\varphi\, d\theta \quad (15)$$

where $r_{CW} = r_{CW}(R',r,\varphi) = (R'^2 + r^2 - 2rR'\cos\varphi)^{1/2}$ is the distance from the center of the cation to a water molecule a distance r from the molecule located at R'. The upper limit of the second integral, $\varphi_2 = \varphi_2(R',r)$, is given by

$$\varphi_2 = \pi, \quad r \le R_0 - R'$$

$$\varphi_2 = \varphi_2(r,R'), \quad r > R_0 - R' \quad (16)$$

where

$$\varphi_2(r,R') = \cos^{-1}\left\{\frac{R'^2 + r^2 - R_0^2}{2rR'}\right\} \quad (17)$$

and where R_0 is the location of the first minimum in $g_{CW}^{com}(r)$. To obtain values for $g_{CW}^{com}(r)$ at arbitrary r, we interpolated the region of $g_{CW}^{com}(r)$ on $[R_x,R_0]$ with a polynomial. We also have the volume of the spherical shell at r

$$v^{shell}(r)|_{R'}\, 2\pi \int_0^{\varphi_2}\int_{r-dr/2}^{r+dr/2} r^2\, dr \sin\varphi\, d\varphi \quad (18)$$

and the number density of water in the shell

$$\rho_b^{shell}|_{R'} = \frac{n_b^{shell}(r)}{v^{shell}(r)}|_{R'} \quad (19)$$

The value of R' is not fixed but takes on values that are distributed according to $g_{CW}^{com}(r)$. Finally, the radial distribution function between two water molecules restricted to the same solute solvation shell is defined by

$$g^{shell}(r) = \frac{\langle n^{shell}(r)\rangle}{\langle n_b^{shell}(r)\rangle_{R'}} \quad (20)$$

where $\langle\ \rangle$ represents an ensemble average and $n^{shell}(r)$ is the number of water molecules a distance r apart which are both in the first solvation shell of the cation.

References and Notes

(1) Kauzmann, W. *Adv. Protein Chem.* **1959**, *14*, 1.
(2) Franks, F. In *Water: A Comprehensive Treatise*; Franks, F., Ed.; Plenum: New York, 1975; Vol. 4, Chapter 1.
(3) Franks, F., Ed. *Water: A Comprehensive Treatise*; Plenum: New York, 1973; Vol. 2.
(4) Franks H. S.; Evans, M. W. *J. Chem. Phys* **1945**, *13*, 507.
(5) McMullan, R.; Jeffrey, G. A. *J. Chem. Phys.* **1959**, *31*, 1231.
(6) McMullan, R.; Jeffrey, G. A. *J. Chem. Phys.* **1963**, *39*, 3295.
(7) Wen, W.-Y. *J. Solution Chem.* **1973**, *2*, 253.
(8) Wen, W.-Y. In *Water and Aqueous Solutions*; Horne, R. A., Ed.; Wiley: New York, 1972, Chapter 15, p 613.
(9) Calmettes, P.; Kunz, W.; Turq, P. *Physica B* **1992**, *180&181*, 868.
(10) Hertz, H. G.; Lindman, B.; Siepe, V. *Ber. Bunsen-Ges. Phys. Chem.* **1969**, *73*, 542.
(11) Wen, W.-Y.; Nara, K. *J. Phys. Chem.* **1967**, *71*, 3907.
(12) Wen, W.-Y.; Nara, K.; Wood, R. H. *J. Phys. Chem.* **1968**, *72*, 3048.
(13) Ramanathan, P. S.; Krishnan, C. V.; Friedman, H. L. *J. Solution Chem.* **1972**, *1*, 273.
(14) Xu, H.; Friedman, H. L.; Raineri, F. O. *J. Solution Chem.* **1991**, *20*, 739.
(15) Kunz, W.; Calmettes, P.; Cartailler, T.; Turq, P. *J. Chem. Phys.* **1993**, *99*, 2074.
(16) Lü, H.; Leaist, D. G. *J. Solution Chem.* **1991**, *20*, 199.
(17) Green, J. L.; Sceats, M. G.; Lacey, A. R. *J. Chem. Phys.* **1987**, *87*, 3603.
(18) Kęcki, Z.; Dryjański, P. *J. Mol. Struct.* **1992**, *275*, 135.
(19) Eriksson, P.-O.; Lindblom, G.; Burnell, E. E.; Tiddy, G. J. T. *J. Chem. Soc., Faraday Trans. 1* **1988**, *84*, 3129.
(20) Giuliano A.; Tani, A. *J. Chem. Phys.* **1980**, *72*, 580.
(21) Geiger, A.; Rahman, A.; Stillinger, F. H. *J. Chem. Phys.* **1979**, *70*, 263.
(22) Guillot, B.; Guissani, Y.; Bratos, S. *J. Chem. Phys.* **1991**, *95*, 3643.
(23) Owicki J. C.; Scheraga, H. A. *J. Am. Chem. Soc.* **1977**, *99*, 7413.
(24) Swaminathan, S.; Harrison, S. W.; Beveridge, D. L. *J. Am. Chem. Soc.* **1978**, *100*, 5705.
(25) Tanaka, H.; Nakanishi, K.; Touhara, H. *J. Chem. Phys.* **1984**, *81*, 4065.
(26) Re, M.; Laria, D.; Fernández-Prini, R. *Chem. Phys. Lett.* **1996**, *250*, 25.
(27) Besseling, N. A. M.; Lyklema, J. *Pure Appl. Chem.* **1995**, *67*, 881.
(28) Lazaridis T.; Paulaitis, M. E. *J. Phys. Chem.* **1992**, *96*, 3847.
(29) Turner, J. Z.; Soper, A. K.; Finney, J. L. *J. Chem. Phys.* **1995**, *102*, 5438.
(30) Finney J. L.; Turner, J. *Faraday Discuss. Chem. Soc.* **1988**, *85*, 125.
(31) Turner, J.; Soper, A. K.; Finney, J. L. *Mol. Phys.* **1990**, *70*, 679.
(32) Turner, J.; Soper, A. K.; Finney, J. L. *Mol. Phys.* **1992**, *77*, 411.
(33) Turner, J.; Soper, A. K.; Finney, J. L. *Mol. Phys.* **1992**, *77*, 431.
(34) Turner J.; Soper, A. K. *J. Chem. Phys.* **1994**, *101*, 6116.
(35) Mezei, M.; Beveridge, D. L. *J. Chem. Phys.* **1981**, *74*, 622.
(36) Berendsen, H. J. C.; Postma, J. P. M.; van Gunsteren, W. F.; Hermans, J. In *Intermolecular Forces: Proceedings of the Fourteenth Jerusalem Symposium on Quantum Chemistry and Biochemistry*; Pullman, B., Ed.; Reidel: Dordrecht, The Netherlands, 1981; pp 331−342.
(37) Jorgensen W. L.; Gao, J. *J. Phys. Chem.* **1986**, *90*, 2174.
(38) Ryckaert, J.-P.; Bellemans, A. *Discuss. Faraday Soc.* **1978**, *66*, 95.
(39) Böcker, J.; Schlenkrich, M.; Bopp, P.; Brickmann, J. *J. Phys. Chem.* **1992**, *96*, 9915.
(40) Pálinkás, G.; Riede, W. O.; Heinzinger, K. *Z. Naturforsch.* **1977**, *32A*, 1137.
(41) Slusher J. T.; Cummings, P. T. *Mol. Simulat.* **1996**, *18*, 213.
(42) De Leeuw, S. W.; Perram, J. W.; Smith, E. R. *Proc. R. Soc. London*, **1980**, *A373*, 27.
(43) De Leeuw, S. W.; Perram, J. W.; Smith, E. R. *Proc. R. Soc. London*, **1980**, *A373*, 57.
(44) Melchionna, S.; Ciccotti G.; Holian, B. *Mol. Phys.* **1993**, *78*, 533.
(45) Allen M. P.; Tildesley, D. J. *Computer Simulation of Liquids*, Oxford University: New York, 1987.
(46) Geist, A.; Beguelin, A.; Dongarra, J.; Jiang, W.; Manchek, R.; Sunderam, V. *PVM 3 User's Guide and Reference Manual*; ORNL/TM-12187, 1994.
(47) Slusher, J. T.; Decker, K. J.; Liu, H.; Vega, C. A.; Cummings, P. T.; O'Connell, J. P. *J. Chem. Eng. Data* **1994**, *39*, 506.
(48) Slusher, J. T.; Cummings, P. T.; Hu, Y.; Vega, C. A.; O'Connell, J. P. *J. Chem. Eng. Data* **1995**, *40*, 792.
(49) Bradl, S.; Lang, E. W.; Turner, J. Z.; Soper, A. K. *J. Phys. Chem.* **1994**, *98*, 8161.
(50) Sceats M. G.; Rice, S. A. *J. Chem. Phys.* **1980**, *72*, 3236.
(51) Chialvo A. A.; Cummings, P. T. *J. Phys. Chem.* **1996**, *100*, 1309.
(52) Bradl S.; Lang, E. W. *J. Phys. Chem.* **1993**, *97*, 10463.
(53) Easteal A. J.; Woolf, L. A. *J. Solution Chem.* **1986**, *15*, 1003.
(54) General discussion: *Faraday Discuss. Chem. Soc.* **1988**, *85*, 147.
(55) Buckner, J. K.; Jorgensen, W. L. *J. Am. Chem. Soc.* **1989**, *111*, 2507.
(56) Diamond, R. M. *J. Phys. Chem.* **1963**, *67*, 2513.
(57) Kreis, R. W.; Wood, R. H. *J. Phys. Chem.* **1971**, *75*, 2319.
(58) Evans, D. F.; Kay, R. L. *J. Phys. Chem.* **1966**, *70*, 366.
(59) Cummings, P. T.; Stell, G. *Mol. Phys.* **1984**, *51*, 253.
(60) Chialvo, A. A.; Cummings, P. T.; Cochran, H. D.; Simonson, J. M.; Mesmer, R. E. *J. Chem. Phys.* **1995**, *103*, 9379.
(61) Reed, T. M.; Gubbins, K. E. *Applied Statistical Mechanics*; Butterworth-Heinemann: Boston, 1973.
(62) Stillinger, F. H. *J. Solution Chem.* **1973**, *2*, 141.
(63) Postma, J. P.; Berendsen, H. J.; Haak, J. R. *Faraday Symp. Chem. Soc.* **1982**, *17*, 55.
(64) Zichi, D. A.; Rossky, P. J. *J. Chem. Phys.* **1985**, *83*, 797.
(65) Ashbaugh, H. S.; Paulaitis, M. E. *J. Phys. Chem.* **1996**, *100*, 1900.